Journal of Magnetic Resonance 214 (2012) 166–174

Contents lists available at SciVerse ScienceDirect

Journal of Magnetic Resonance

journal homepage: www.elsevier.com/locate/jmr

A multi-sample 94 GHz dissolution dynamic-nuclear-polarization system

Michael Batel [a,2], Marcin Krajewski [b,2], Kilian Weiss [b], Oliver With [a], Alexander Däpp [a], Andreas Hunkeler [a], Martin Gimersky [c,1], Klaas P. Pruessmann [b], Peter Boesiger [b], Beat H. Meier [a], Sebastian Kozerke [b,*], Matthias Ernst [a,*]

[a] Physical Chemistry, ETH Zürich, Wolfgang-Pauli-Strasse 10, 8093 Zürich, Switzerland
[b] Institute for Biomedical Engineering, University and ETH Zürich, Gloriastrasse 35, 8092 Zürich, Switzerland
[c] Laboratory for Electromagnetic Fields and Microwave Electronics, ETH Zürich, Gloriastrasse 35, 8092 Zürich, Switzerland

ARTICLE INFO

Article history:
Received 3 October 2011
Revised 4 November 2011
Available online 15 November 2011

Keywords:
Dynamic nuclear polarization
Dissolution DNP
Multi-sample DNP
Hyperpolarization
Longitudinal detection EPR (LOD)
Hardware

ABSTRACT

We describe the design and initial performance results of a multi-sample dissolution dynamic-nuclear-polarization (DNP) polarizer based on a Helium-temperature NMR cryostat for use in a wide-bore NMR magnet with a room-temperature bore. The system is designed to accommodate up to six samples in a revolver-style sample changer that allows changing samples at liquid-Helium temperature and at pressures ranging from ambient pressure down to 1 mbar. The multi-sample setup is motivated by the desire to do repetitive *in vivo* measurements and to characterize the DNP process by investigating samples of different chemical composition. The system can be loaded with up to six samples simultaneously to reduce sample loading and unloading. Therefore, series of experiments can be carried out faster and more reliably. The DNP probe contains an oversized microwave cavity and includes EPR and NMR capabilities for monitoring the DNP process. In the solid state, DNP enhancements corresponding to ~45% polarization for [1-^{13}C]pyruvic acid with a trityl radical have been measured. In the initial liquid-state acquisition experiments described here, the polarization was found to be ~13%, corresponding to an enhancement factor exceeding 16,000 relative to thermal polarization at 9.4 T and ambient temperature.

1. Introduction

The inherently low sensitivity is a major drawback of nuclear magnetic resonance spectroscopy and magnetic resonance imaging and leads to long measurement times. At typical magnetic fields of several Tesla and at room temperature, the polarization of the Zeeman system is only on the order of 10^{-5} (10,001 up spins compared to 10,000 down spins). This is a problem, for example, in spatially-resolved magnetic resonance spectroscopy where the distribution of metabolic substances in the organism is of interest. The large background of abundant water protons overwhelms the ^{1}H resonances of potentially interesting substrates in low endogenous concentrations. Magnetically active isotopes other than ^{1}H, e.g., ^{15}N or ^{13}C are difficult to detect with sufficient spatial resolution due to their low natural abundance and lower gyromagnetic ratio.

Various methods to increase the thermal equilibrium polarization have been proposed over the years. Such hyperpolarization techniques include optical pumping of noble gases and semiconductors [1,2], para-hydrogen induced polarization [3,4], the Haupt-effect in methyl groups [5,6], chemically-induced dynamic nuclear polarization [7], and dynamic nuclear polarization using free radicals (DNP) [8]. In DNP, electron polarization is transferred to the nuclei under microwave irradiation of the electron spins. At temperatures around 1–2 K which are easily reachable in a DNP apparatus, the electron polarization reaches almost 100%. Ardenkjaer-Larsen et al. [9] extended the DNP method from applications at cryogenic solid-state conditions to applications at room-temperature liquid-state conditions using fast dissolution of the solid sample by hot water. This idea made polarization enhancement by DNP applicable to *in vivo* applications after injection of the polarized solution into the organism [10], and is referred to as dissolution DNP.

In dissolution DNP, the target samples are glass-forming solutions (50–500 μl) containing the target molecule and an organic stable free radical like TEMPO or trityl. Typical polarization levels of the target nuclei (e.g., ^{13}C) can reach up to 50% by transfer of polarization from the almost fully polarized electron spin. Subsequently, the hyperpolarized sample is rapidly dissolved and transferred to

* Corresponding authors.
E-mail addresses: kozerke@biomed.ee.ethz.ch (S. Kozerke), maer@ethz.ch (M. Ernst).
[1] Present address: Astrium Ltd., Secure Satcom Systems, Anchorage Road, Portsmouth PO3 5PU, UK.
[2] These authors contributed equally to this work.

1090-7807/$ - see front matter © 2011 Elsevier Inc. All rights reserved.
doi:10.1016/j.jmr.2011.11.002

the MRI/NMR spectrometer. The polarization enhancements in the dissolved sample have been reported to be larger than a factor of 10,000 [9,11,12] compared to thermal-equilibrium polarization at ambient temperature.

An important application of dissolution DNP is metabolic MRI [10], where a metabolite with hyperpolarized nuclear spins is injected into an organism for *in vivo* tracing of the marker molecule and its metabolic products [13–15]. This procedure opens unprecedented opportunities in MRI. Like most hyperpolarization techniques, the dissolution DNP method is limited by the fact that the high polarization is available only for a time window on the order of T_1. Therefore, it has to be used for the entire experiment due to the slow polarization build-up time of the DNP process.

Several dissolution DNP polarizers based on the same principle structure and functionality have been built recently [16–19]. They consist of a pumped Helium-temperature cryostat with a waveguide for microwave irradiation and a mechanical transfer system for moving the sample into and out of the cryostat. The transfer system accommodates a dissolution apparatus that is used to extract the polarized sample from the cryostat. The polarizer is typically equipped with a simple NMR resonance circuit to determine the nuclear polarization levels. A drawback of this design is that only a single sample can be stored in the polarizer, polarized, and dissolved at a time. After this process, the sample tray has to be unloaded and a subsequent target sample has to be loaded into the cryostat. Therefore, the repetition rate for multiple dissolution DNP experiments is limited by the time needed for changing and polarizing the sample, which is typically 40–90 min.

Decreasing the minimum repetition time between successive dissolution DNP experiments can be important for, e.g., cardiac experiments of repeated ischemia/reperfusion to study conditioning of the heart. Furthermore, the investigation of the dependence of the DNP efficiency on various sample parameters requires serial experiments, which could be simplified by having multiple samples loaded in the polarizer simultaneously. Such a system was recently introduced by Ardenkjaer-Larsen et al. and accommodates up to four samples at a time [20].

In this work, we present the design and performance results of a dissolution DNP polarizer with multi-sample functionality optimized for sequential polarization of up to six samples. The system is intended for the investigation of the dependence of the DNP process on sample parameters as well as for the pre-polarization of multiple samples for repetitive *in vivo* dissolution DNP experiments. A resonant microwave cavity is used to increase the DNP efficiency at low incident microwave power, reducing heating of the sample during microwave irradiation. For monitoring the nuclear polarization during DNP experiments as well as for investigation of the DNP process itself, NMR and EPR capabilities are included in the polarizer. The setup including the cryogenic hardware components was designed to be compatible with wide-bore NMR magnets yielding flexibility in the choice of the polarizer magnet.

2. Instrumentation

The polarizer presented here is based on published principle designs [9,17,21] extended by a multi-sample capability realized with a revolver-like design. The system is based on a Helium-temperature cryostat that is mounted in a 7 T Bruker wide-bore (89 mm) magnet charged to 3.35 T. The multi-sample feature requires the samples to be positioned outside the center axis of the magnet. Since the requirements on field homogeneity for DNP and NMR experiments at liquid-Helium temperatures are limited by the NMR line width (>100 ppm), the field deviation and inhomogeneity within the sample space (<10 ppm) are negligible. The system is shown schematically in Fig. 1 and is controlled with software written in LabVIEW (National Instruments).

2.1. Cryo system

The DNP probe is inserted in a cryo system that consists of a variable temperature insert (VTI), a liquid-Helium transfer line, and vacuum pumps. An ITC-503 controller (Oxford Instruments) is used for temperature regulation.

The VTI is a SpectrostatNMR cryostat (Oxford Instruments) working with a continuous liquid-Helium flow drawn through the transfer line from a liquid-Helium supply dewar. A needle valve controlled by a stepper motor regulates the flow of liquid Helium. Through a capillary, the Helium is guided to the bottom of the cryostat and enters the sample space.

For initial cool-down and for operation at temperatures above 3 K, the cryostat is pumped by an oil-free vane pump (GF4, Oxford Instruments). In this mode, the exhaust gas is pumped through a tube surrounding the Helium-supply capillary within the transfer line. Thereby, the transfer line is precooled by the exhaust Helium gas reducing the overall consumption of liquid Helium.

For temperatures below 3 K, the evaporated Helium is pumped directly through an exhaust port on the cryostat. Large diameter tubing (ISO-KF 40) minimizes the pressure drop along the exhaust line. A roots pump (Okta 250 A, Pfeiffer Vacuum) backed by a rotary vane pump (SV40B, Oerlikon Leybold Vacuum) are used in this mode.

2.2. DNP probe

The core of the dissolution DNP system is the in-house-built DNP probe shown in Fig. 2. It contains the waveguide and cavity needed for microwave irradiation, the NMR and EPR coils, and the sample changer. The design differs considerably from published designs [16,17].

2.2.1. The revolver

The key feature is the "revolver", allowing up to six samples to be loaded, polarized, and dissolved separately. The system allows exchanging the samples at cryogenic temperatures. Polarization,

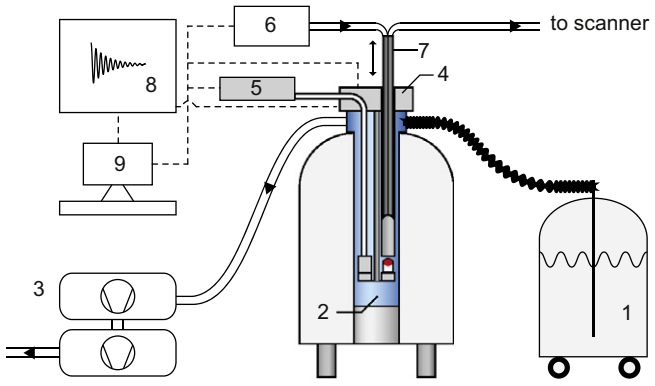

Fig. 1. Schematic drawing of the complete dissolution DNP system. The flow-type cryo system consists of an external liquid-Helium supply dewar (1) connected to the variable-temperature cryostat (2) via a vacuum shielded transfer line. Helium is dragged into the sample space by evacuating the cryostat with two vacuum pumps (3) connected in series. The DNP probe (4) is mounted and sealed to the cryostat within the bore of the magnet. A microwave source (5) is connected to the waveguide leading to the sample space. The dissolution system (6) is attached to the tubing of the dissolution stick (7) for dissolution and shuttling to the nearby NMR/MRI spectrometer. An OPENCORE NMR console (8) is used to monitor the nuclear polarization while the entire system is controlled by LabVIEW software (9). Dotted lines indicate data communication pathways.

Fig. 2. Drawing of the DNP probe developed for dissolution DNP which is inserted into the VTI. The room-temperature top end of the probe holds the vertical (1) and rotational (2) pneumatics for the revolver mechanism, the dissolution-port tube (3) and microwave guide (4) run from there to the cryo space (Fig. 3).

NMR, and EPR measurement can be carried out at the location of the cavity, while sample loading, unloading, and dissolution are performed at a second location. The principal design is shown in Fig. 3. A central shaft is mounted such that it can be rotated and moved up and down, thereby connecting the room-temperature high-pressure top section of the DNP probe with the sample area. At the lower end, a platform is attached featuring six equivalent sample holders. Each holder is a bottom-closed cylinder forming the lower half of the microwave cavity. The design exhibits a rotational symmetry that is broken by two unique sites that are at fixed positions within the probe: the top part of the microwave cavity and the dissolution port located opposite one another with respect to a rotation of the revolver. This leads to six distinct revolver positions in which one of the six samples is in the cavity and another sample in the dissolution-port position.

Sample changing is achieved by sequential lowering of the movable bottom platform, rotating by multiples of 60°, and pulling the platform back up. In each position, one of the six bottom-closed cylinders closes the cavity, resulting in a resonant microwave structure.

2.2.2. Microwave cavity

The microwave cavity is designed with two goals in mind: First, to effectively use the microwave power, allowing for cost-effective sources, the quality factor (Q) of the resonant cavity should be high, and second, to reduce heating, the excited microwave magnetic field should be concentrated within the sample volume and – at the same time – the electric field at the location should be minimized to avoid direct sample heating. While the latter cannot be fully achieved for sample sizes larger than the microwave wavelength, oversized (multi-mode) cavities allow the available microwave power to be concentrated at the sample location. The cavity used in our DNP setup (Fig. 4a) has been optimized, using numerical simulations (CST Microwave Studio), to maximize and homogenize the fields within the sample volume (Fig. 4b). For this

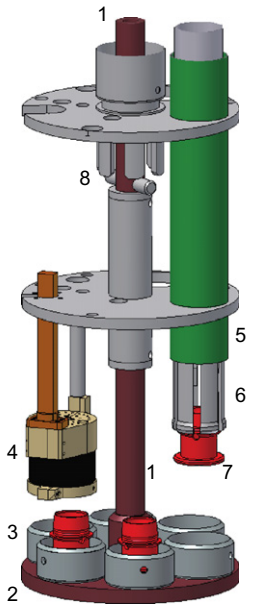

Fig. 3. The revolver-style lower end of the DNP probe. The rotationally and vertically movable axis (1) connects the room-temperature space to the sample holder platform (2). Six bottom-closed cylinders (3) can be combined with the top part of the cavity (4) to form the resonant microwave structure. The dissolution port (5) runs from room-temperature to the sample space guiding the grabber (6) to reach the sample cups (7). A pin-in-channel system (8) guides the revolver mechanism to open, rotate, and close to the correct positions.

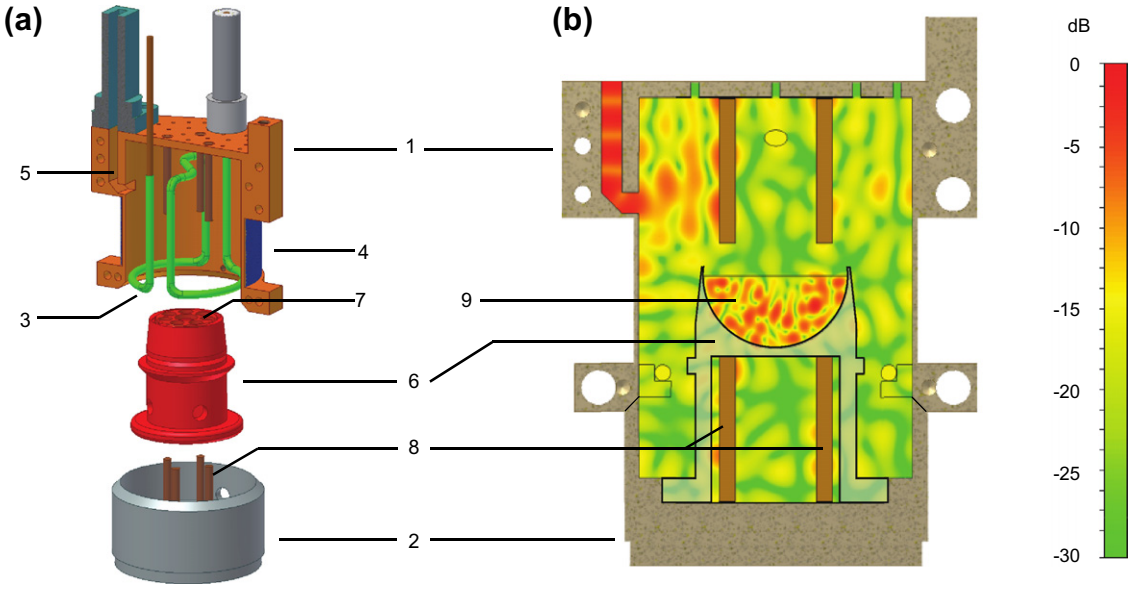

Fig. 4. (a) The microwave cavity. Top (1) and bottom (2) part of the oversized resonant microwave structure, NMR coil (3), EPR coil (4), microwave guide inlet (5), sample cup (6) with closing lid (7), and brass rods (8) for optimizing the microwave field and stabilizing of the sample cups. (b) Cross section through the microwave cavity. Overlaid is the simulated normal component of the microwave B-field, plotted in dB units with respect to the maximum B-field found at the entrance of the microwave guide into the cavity. The metallic rods (8) promote the homogenization and concentration of the microwaves in the sample space (9).

purpose, eight metallic rods are placed inside the cavity. The four located in the lower part of the cavity additionally facilitate accurate positioning of the sample cup.

The cavity shown in Fig. 4 is built from non-magnetic brass and composed of an upper and lower part such that it can be opened for changing the samples. To ensure correct closing of the cavity, the six lower halves are mounted on sapphire beads acting as spherical bearings (<100 μm play). Correct functioning of the closing mechanism is checked using a vertical lift monitor (Section 2.2.5).

The cavity also contains an NMR saddle-coil that is compatible with the revolver mechanism. For monitoring of the EPR spectrum under DNP conditions, a solenoid EPR coil was wound on the outer surface of the cavity to enable longitudinal detection of EPR [22]. This technique, as described in the following section, utilizes modulation frequencies in the range of 1 kHz. In the area of the EPR coil, the brass wall was chosen to be only 400 μm thin, below 10% of the skin depth of brass at the frequency of 1 kHz.

2.2.3. EPR circuit and microwave source

The apparatus is designed to record the EPR line shape under DNP conditions. We have implemented a setup that uses longitudinal detection (LOD) [22,23] as demonstrated for a dissolution DNP system by Granwehr et al. [21]. In LOD experiments, amplitude modulation of continuous-wave (CW) microwave irradiation can be used to periodically saturate the electron magnetization. The resulting time-dependent longitudinal magnetization then induces an alternating voltage in the EPR coil. Further discussions considering dependencies on electron spin–lattice relaxation times, microwave power, and modulation amplitude and frequency can be found in literature [24–26].

The general microwave setup chosen is shown schematically in Fig. 5 and consists of four subunits. A computer for signal controlling and detection, a data acquisition and signal generation device, a microwave source with variable power, and the detection circuit. On the controlling computer, a periodic signal is generated for amplitude modulation and homodyne detection of the LOD signal using a NI data acquisition (DAQ) device (NI USB-6229 DAQ). The amplitude modulation signal is supplied by the DAQ digital to analog converter, amplified and fed to the microwave power attenuator.

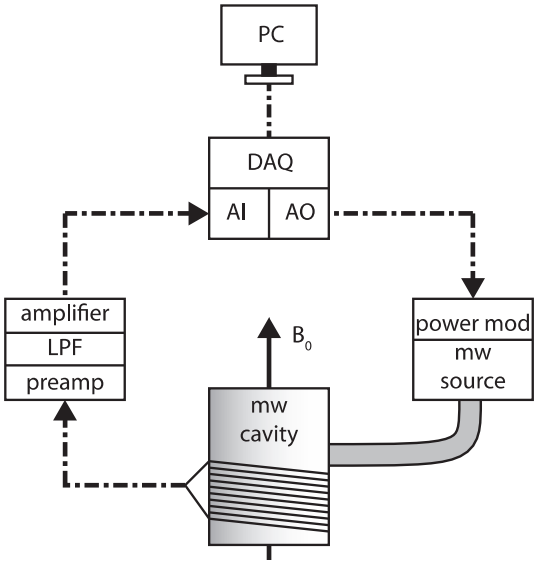

Fig. 5. Schematic drawing of microwave and LOD circuit. The microwave power modulation signal is generated in LabVIEW, converted to an analog signal by the DAQ and send to the microwave source power attenuator. The LOD signal acquired by the EPR coil on the cavity is amplified, low-pass filtered, and fed to the DAQ for digitization and processing in LabVIEW.

The microwave source (Model VCOM-10/94/200-DD, ELVA-1) can provide up to 180 mW of CW power at frequencies between 93.75 and 94.25 GHz and features a voltage-controlled power attenuator (0–40 dB). For amplitude-modulated LOD experiments, the microwave source is operated in CW mode with the analog amplitude modulation signal fed to its power attenuator. The switching time was measured to be approximately 100 μs.

The EPR detection circuit consists of a copper coil (380 turn and 100 μm diameter wire) aligned parallel to the B_0 field. The circuit is non-resonant and well insulated from ground to minimize cross

talk with the power-modulation signal. The coil is connected in differential mode to an audio preamplifier (SSM2019) followed by an active 50 kHz low-pass filter preventing high-frequency noise to be aliased during data sampling.

2.2.4. NMR circuit

For monitoring the nuclear polarization levels during DNP experiments, an NMR coil is incorporated into the DNP probe. It allows NMR experiments at all operating temperatures. The circuit has a two-stage tuning and matching design. A first fixed pre-tuning in the cold space is achieved above the cavity by a series capacitor generating a series LC circuit with the NMR coil. A second fine-tuning and matching unit is located at the top of the probe at room temperature. A semi-rigid RF transmission line connects the two tuning stages. The NMR saddle coil with two effective windings is mounted inside the upper part of the microwave cavity (Fig. 4a). The NMR experiments are controlled by an OPENCORE NMR console [27] with an in-house-built LabVIEW interface.

2.2.5. Sensor system

The DNP system is equipped with several sensors to control its performance and to monitor the status of the DNP experiments. All sensor readings are fed to the LabVIEW control software. Two temperature sensors (Cernox resistors, Lake Shore Cryotronics Inc.) are mounted inside the polarizer. One is located on the bottom of the cryostat. The other one is mounted on the outside of the microwave cavity at the height of the sample location. Both sensors are read out by the ITC temperature controller.

To monitor the level of liquid Helium in the cryostat, a cylindrical capacitor is mounted at the lower end of the DNP probe. It consists of two 80 mm long coaxial cylindrical electrodes with a diameter of 2.88 and 2 mm, respectively. Liquid Helium can enter the structure, acting as a dielectric medium and changing the capacitance. The capacitance is measured by a capacitance-to-digital converter (AD7746, Analog Devices).

A pressure sensor is mounted at the vacuum port of the cryostat to estimate the system pressure (Series P3301, tecsis GmbH). This sensor cannot be utilized for temperature calibration of the sample during cryogenic operation since a pressure drop of unknown magnitude builds up between the lower part and the vacuum port of the cryostat. The analog voltage signal is digitized using the voltage input channel of the capacitance-to-digital converter.

The correct operation of the revolver-style sample changer is monitored by a sensor subsystem. It consists of three phototransistors for digital decoding of the actual revolver position into TTL signals, two switches (TTL) for assuring correct functionality of the revolver pneumatics, and an in-house-built vertical lift monitor. The analog voltage output of the lift monitor allows measurement of the vertical movement of the revolver axis with a resolution of ~50 μm. All revolver sensors are mounted at the top end of the probe, avoiding heating of the sample space.

2.2.6. Sample cups and grabber

The frozen samples sit in sample cups shown in Figs. 3 and 4. The geometry of the cups is defined by following characteristics: The sample area is a semi-spherical shape with a volume of 150 μl giving an effective load volume of 100 μl, assuming a packing factor of approximately 70%. The cup is closed by a perforated lid permitting the dissolution medium to penetrate during dissolution. The lid prevents frozen sample beads from being jolted out of the cup during movement of the revolver or due to boiling Helium. The lower sections of the cups are hollow and clasp around the bottom four metallic rods of the microwave cavity. The upper outer shape of the cup is cone-like with a decreasing diameter towards the top. This geometry enables the dissolution stick, with fitting shape, to seal the cup when being pressed on it. Finally, the grabber locks into a circular channel in the side of the cup for loading and dissolution purposes.

The grabber, shown in Fig. 6a, is used to grab and steady the sample cups. It consists of a hollow tube with double-layer structure. The outer layer ends in six fingers, each having hooks pointing inwards to lock into the circular channel of the sample cups. The inner tube can be moved in and out to open and close the fingers of the grabber. The grabber is utilized for fixing and lifting of the cups during dissolution and for loading sample cups through the dissolution port. This can be done during system temperatures as low as 4.2 K at ambient pressure.

2.3. Dissolution and shuttling components

The dissolution apparatus is based on a design described previously [16]. The main hardware components are: (i) a 10 ml stainless-steel vessel that can be pressurized and heats the dissolution medium (usually a buffered solution) to 160 °C, (ii) a system of valves for pre-pressurizing, starting the dissolution, and shuttling of the dissolved sample to the MRI/NMR system, (iii) a dissolution stick (Fig. 6b) to guide the hot dissolution medium to the sample space through a PTFE tube connected to the cooker. The dissolution stick has to be sealed tightly to the sample cup. This seal prevents the hot liquid from entering the cryo-temperature space. The dissolved sample is guided out of the polarizer through a second PTFE tube in the dissolution stick. The usage of (iv) a collecting device next to the DNP magnet or at the MRI/NMR system will not be discussed here. The type of device used depends on the application the polarized dissolved sample is used for. (v) Temperature and pressure sensors monitor the functionality of the dissolution system. All valves and sensors are controlled by the LabVIEW software.

3. Performance and results

In this section we describe operation procedures and performance of the main components of our DNP system.

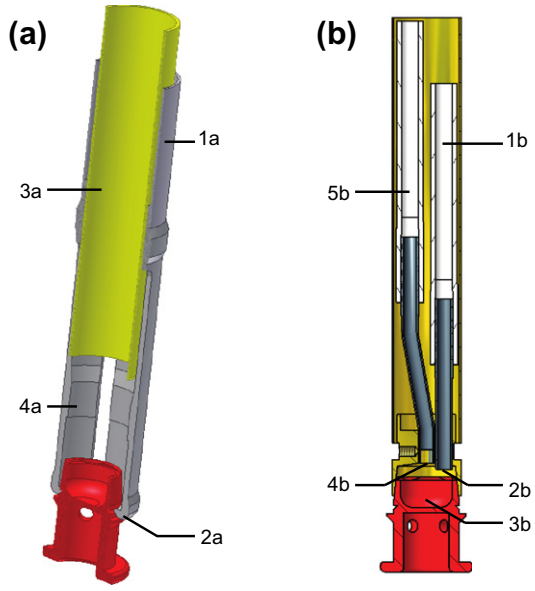

Fig. 6. (a) The grabber. The outer tube (1a) of the 2-layer structure ends in six fingers with hooks (2a) for "grabbing" the cups. The inner layer (3a) can be longitudinally slid to open the fingers by pushing against their spreader (4a). (b) The dissolution stick sealed to a sample cup. A PTFE tube (1b) guides the dissolution medium to the dissolution inlet (2b) at the sample space (3b). Through the outlet (4b) the dissolved medium is guided to the room-temperature space by a second PTFE tube (5b).

3.1. Cryogenic performance

The initial cool-down of the system to below liquid-Helium temperature is conducted by pumping on the cryostat through the transfer line exhaust tube with a fully opened needle valve for the liquid-Helium supply. This takes approximately 50 min and uses 6 l of liquid Helium. The system can be operated in three cryogenic modes:

1. For inter-experimental periods, e.g., over-night parking, the system is kept at 20–80 K by weakly pumping on the transfer line exhaust tube with the Helium-supply needle valve opened 8–15%. In this mode the cryogenic consumption is below 0.4 l of liquid Helium per hour.
2. In "continuous mode", the Helium needle valve is kept partially open while the system is pumped to low vacuum. This allows experimental periods of constant low temperatures limited in time only by the liquid-Helium supply dewar. The system reaches temperatures down to 1.9 K with 4 l of liquid Helium per hour.
3. Lowest temperatures are reached in "single-shot" mode. For this mode the cryostat is first filled with liquid Helium. Subsequently, the Helium-supply needle valve is closed and the cryostat pumped to <2 mbar. For microwave irradiation below 30 mW, the system reaches a single-shot temperature of 1.3 K for a maximum duration of 3 h with a liquid-Helium consumption of 0.13 l per hour.

The Helium-supply dewar can be changed at probe temperatures of 4.2 K or higher after pressurizing the cryostat to atmospheric pressure. Samples can also be loaded at temperatures of 4.2 K or higher. The revolver mechanism was found to work at all achievable temperatures and pressures. The samples could be interchanged reliably between cavity and dissolution port at any time during the DNP experiments. To prevent traces of contamination gases from freezing and blocking the revolver mechanism after initial loading of multiple samples, the system is heated to 80 K and evacuated for 5 min.

3.2. Solid-state DNP

All experiments below 4.2 K were performed while keeping the liquid-Helium level in the cryostat above sample height to assure efficient sample cooling. DNP experiments were conducted on a sample with 16.2 mM trityl radical (tris (8-carboxyl-2,2,6,6-tetra(2-(1-hydroxyethyl))-benzo[1,2-d;4,5-d']bis(1,3)dithiole-4-yl) methyl sodium salt), 1 mM Gd (Gadovist, Bayer HealthCare) dissolved in [1-^{13}C]pyruvic acid (ISOTEC/Sigma–Aldrich). Before switching to the single-shot mode, the system was kept at constant 3.45 K for 60 min to measure a thermal-equilibrium reference spectrum. The relaxation time of the ^{13}C signal at this temperature was about 400 s. After reaching the single-shot temperature of 1.4 K, the sample was irradiated for 60 min until reaching the polarization plateau. The microwave frequency and power were previously optimized and set to 93.875 GHz and 20 mW, respectively (Figs. 7 and 9). Low-flip angle (~4°) one-dimensional ^{13}C NMR spectra were acquired over the entire course of experiment to determine the amount of ^{13}C polarization. The integrated NMR intensities were compared to the measured average thermal-equilibrium signal and translated into polarization using the measured thermal-equilibrium ^{13}C polarization at 3.45 K as a reference. The polarization build-up curve was fitted with a mono-exponential curve yielding a polarization at the plateau of 45 ± 5% with a build-up constant of 670 ± 20 s (Fig. 8). The efficiency of the DNP process is shown in Fig. 9 where the plateau polarization is plotted as a function of the microwave power (circles and dashed lines).

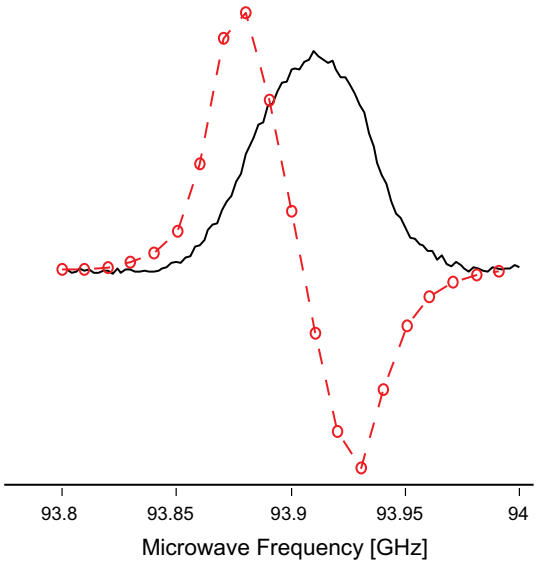

Fig. 7. ^{13}C DNP enhancement (dashed line) as a function of the microwave irradiation frequency overlaid with the LOD EPR spectrum (solid line) of 16 mM trityl in [1-^{13}C]pyruvic acid. The LOD spectrum was acquired at 10 K, the DNP enhancement curve at 3.47 K. The positive DNP maximum was found at 93.875 GHz, which is unchanged at 1.3 K.

One can see that the maximum polarization is already reached for a microwave power around 10-20 mW.

3.3. Cavity efficiency

An additional NMR probe was built that can be inserted into the dissolution port to conduct NMR experiments on the sample cup in the dissolution-port position. This "NMR stick" is a 6 mm outer diameter semi-rigid RF transmission line (both conductors Cu) with a vacuum-tight sealing to the top end of the dissolution port. An NMR saddle coil allows free movement of the sample revolver system. With the NMR stick, DNP experiments where conducted on samples outside the cavity to compare the DNP efficiency inside and outside the cavity. For the same sample as discussed above (16.2 mM trityl, 1 mM Gd in [1-^{13}C]pyruvic acid) the dependence of the polarization levels on the microwave power was measured at 1.4 K inside the closed cavity and outside the opened cavity.

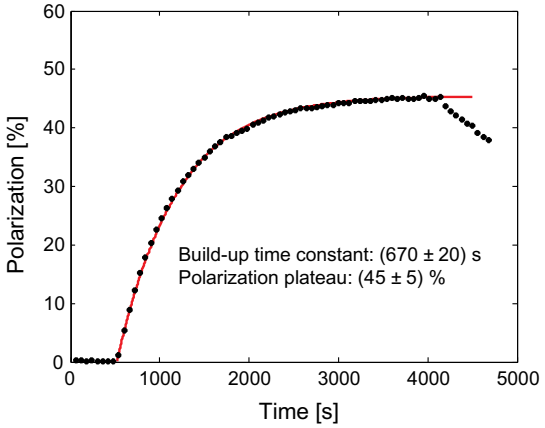

Fig. 8. Solid-state ^{13}C polarization as a function of the microwave irradiation time. The sample contained 16.2 mM trityl and 1 mM Gd in [1-^{13}C]pyruvic acid at a temperature of 1.4 K. At time t = 500 s, the microwaves were switched on with a power setting of 20 mW.

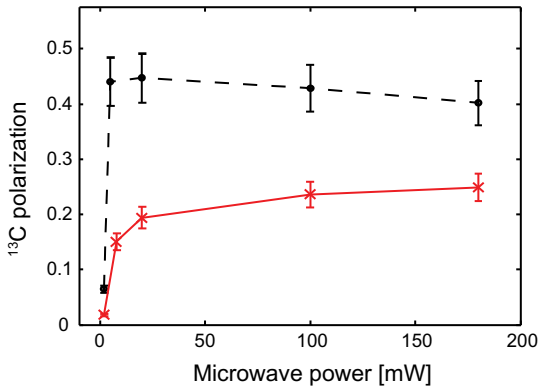

Fig. 9. Dependence of the steady-state solid-state ^{13}C DNP polarization inside the cavity (circles) and in the dissolution-port position with opened cavity (crosses) as a function of the microwave power.

Fig. 9 shows the DNP efficiencies for both experiments. The polarization inside the cavity decreases with power levels above 20 mW. At 180 mW of microwave power the temperature of the sensor on the cavity shows an increase of 0.23 K (17%) compared to the temperature at a microwave power of 20 mW. The polarization profile for the sample outside the cavity shows that the saturation condition is not yet reached at a microwave power of 180 mW where the polarization reaches only 25%.

3.4. EPR experiments

The LOD signal intensity is proportional to the first time derivative of the electron magnetization, i.e., the electron longitudinal relaxation rate and the saturation efficiency. LOD EPR measurements were conducted on a sample containing 50 mM TEMPO (2,2,6,6-Tetramethylpiperidine-1-oxyl, Sigma Aldrich) in 1/1 D_2O/Glycerol at temperatures between 1.3 K and 71 K. Fig. 10 shows the signal-to-noise ratio (SNR) for equal acquisition parameters as a function of the sample temperature (675 Hz saturation frequency, 51 points per spectrum, 377 s of acquisition time per spectrum). The SNR per 377 s of acquisition time at 2 K equals one, making LOD measurements during exact DNP conditions impractical. The reason for this decrease in SNR is the dependence of the LOD signal on the longitudinal relaxation-rate constant of the electron. Below liquid-Helium temperatures, the relaxation time constant increases to values larger than the inverse of the microwave modulation frequency used. The consequence is a steady-state electron longitudinal magnetization close to zero with only small changes during power modulation, resulting in a vanishing LOD signal.

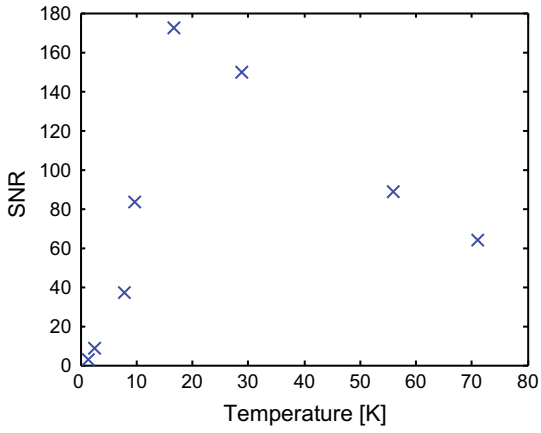

Fig. 10. Temperature dependence of the LOD signal-to-noise ratio for a sample containing 50 mM TEMPO in $(1/1)_{vol}$ D_2O/Glycerol. Equal parameters with 377 s total acquisition time for each LOD experiment.

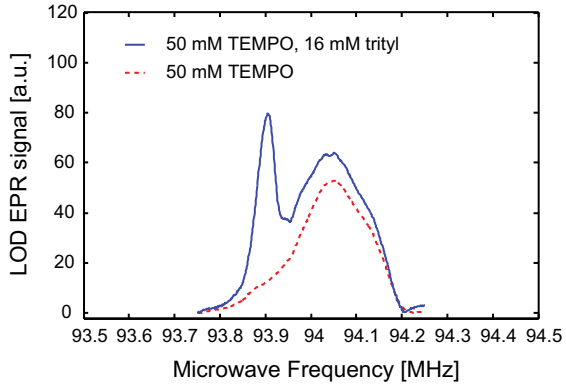

Fig. 11. LOD spectra of 50 mM TEMPO (dotted line) and a mixture 50 mM TEMPO and 16 mM trityl (solid line) both in $(1/1)_{vol}$ D_2O/Glycerol.

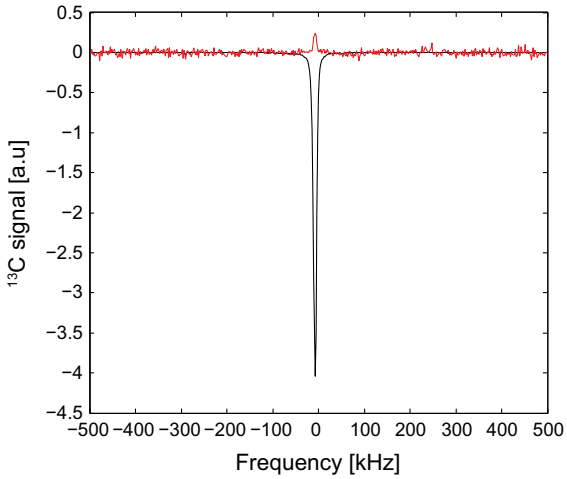

Fig. 12. ^{13}C NMR spectra of a negative DNP enhanced sample at 1.4 K (negative signal) and at thermal equilibrium at 3.47 K scaled by a factor 100 (positive signal). The sample contained 16.2 mM trityl and 1 mM Gd in [1-^{13}C]pyruvic acid. The thermal equilibrium spectrum is the average of 87 spectra, all spectra where acquired with the built-in NMR circuitry of the DNP probe.

Since the shape of the EPR resonance is not expected to change considerably below 10 K, the chosen setup has proven to suffice for EPR measurements close to the DNP conditions. Fig. 11 shows an example of two EPR spectra of the 1/1 D_2O/Glycerol sample containing 50 mM TEMPO (red[3] dotted line) and additional 16 mM trityl (blue solid line).

3.5. NMR experiments

The B_1-field strength on ^{13}C was found to be limited to 10 kHz with a B_1-field homogeneity (FWHH) of ~10 kHz over the sample volume. For the purpose of tracking the NMR enhancements during DNP experiments this is sufficient since low-flip angle experiments are utilized to avoid saturation of the NMR signal.

^{13}C NMR spectra were acquired at room temperature as well as at cryogenic temperatures down to 1.3 K. Fig. 12 shows ^{13}C spectra

[3] For interpretation of color in Figs. 1–12, the reader is referred to the web version of this article.

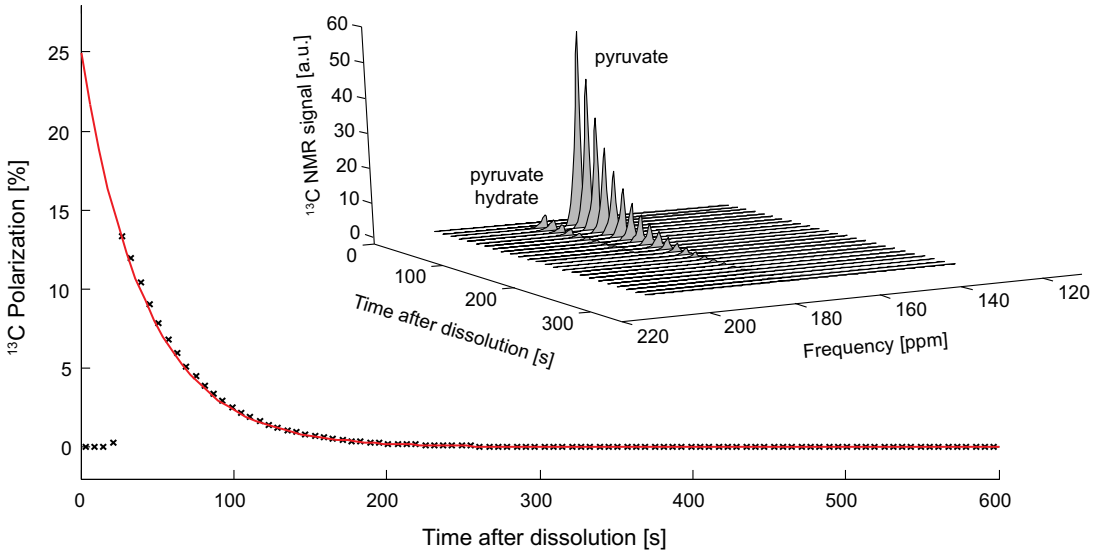

Fig. 13. DNP enhanced ^{13}C polarization in the liquid state at room temperature in a 9.4 T MRI. The inlay shows the time series of low-flip angle 1D ^{13}C spectra of the hyperpolarized [1-^{13}C]pyruvic acid dissolved in 4 ml Tris-buffer with a final pH = 8.

of the sample used for solid-state DNP experiments (16.2 mM trityl, 1 mM Gd in [1-^{13}C]pyruvic acid) at 3.47 K (scaled by a factor 100) and 1.4 K. The spectrum at 3.47 K is the signal average of 87 spectra taken at thermal equilibrium with a repetition time of 30 s. The spectrum at 1.4 K is taken after 50 min of DNP build-up at the optimum microwave frequency for negative DNP. All spectra were acquired with four averaged pulse-acquire experiments with a combined effective flip-angle of 4°. The full width at half maximum in both shown spectra is 7 kHz or 200 ppm, more than 20 times the B_0-field homogeneity of <10 ppm within the sample space.

3.6. Dissolution DNP

For dissolution of a hyperpolarized sample, the target sample cup has to be rotated to the dissolution-port position of the revolver. Dissolution and ejection of the sample involves pressurizing the system to ambient pressure. Then the grabber is employed to hold the target sample cup and lift it above the liquid-Helium bath. The dissolution stick is slid into the hollow sample grabber and sealed against the sample cup with a locking mechanism. The dissolution medium with the dissolved sample can be shuttled to the liquid-state MRI/NMR system by blowing room-temperature Helium gas after dissolution through the entire dissolution line or collected immediately next to the DNP magnet.

For performance tests, the DNP system was installed next to a 7 T NMR spectrometer. A 140 µl sample of [1-^{13}C]pyruvic acid doped with 15 mM trityl was polarized at optimum positive DNP microwave frequency with 20 mW for 60 min at 1.3 K. After reaching the DNP enhancement plateau as monitored by ^{13}C NMR spectroscopy, the dissolution sequence was started following the procedure described above. With a delay of 30 s between sample rotation and dissolution due to initial leak tightness tests, the sample was dissolved in 8 ml D_2O.

The solution was shuttled over a distance of 4 m through PTFE tubing (3 mm inner diameter) into an NMR tube mounted in a standard solution-state probe in the 7 T spectrometer. The shuttling time until arrival of the main bolus is estimated to be less than 5 s. Low-flip angle 1D ^{13}C spectra were acquired in the NMR spectrometer with a repetition time of 6.65 s. The integral over the pyruvate resonance, normalized by the thermal equilibrium signal yields an enhancement factor of 15,000 (or 9.3% ^{13}C polarization at 295 K and a magnetic field of 7 T).

In combination with a 9.4 T MRI system (Bruker BioSpec) dissolution experiments were performed on samples containing 25 µl [1-^{13}C]pyruvic acid doped with 13.5 mM trityl and 1.5 mM Gd (Dotarem, Guerbet) yielding similar solid-state polarizations as shown in Fig. 8. The dissolution workflow was optimized to reduce the exposure of the polarized sample to high-temperature dissolution components and the time between sample rotation and dissolution was minimized. The sample was dissolved in 4 ml Tris-buffer and collected in a syringe where it was mixed with 250 µl of a 1 M NaOH solution to yield pH = 8. The dissolved solution was carried to the MRI system and injected into a phantom. The sample entered the phantom 27 s after dissolution and was measured with low-flip angle (<10°) one-dimensional ^{13}C spectra. The inset in Fig. 13 shows the interesting part of the spectra. The highest measured liquid-state ^{13}C DNP enhancement was calculated to be greater than 16,000 (13% polarization at 295 K and 9.4 T). Assuming the measured T_1 of the dissolved sample (42.3 s) to be constant between the time of dissolution and the arrival in the MRI system, the liquid-state polarization can be extrapolated to be greater than 25% (enhancement factor >30,000) immediately after dissolution, as is plotted in Fig. 13. This corresponds to a loss of polarization during the shuttling of 44%. Reasons for the polarization loss during dissolution other than relaxation due to exposure of the frozen solid to warm components are not known. The few reported values in the literature range from 20% to 45% loss during dissolution [9,17].

4. Discussion and conclusion

The design principles and the basic functionality of a dissolution DNP system have been presented. The system is designed to fit a wide-bore NMR magnet with a room-temperature bore.

The performance tests of the microwave circuit have demonstrated that the microwave magnetic field is effectively concentrated at the sample location requiring only 10-20 mW of microwave power measured at the microwave source for reaching maximum DNP enhancements.

The multi-sample revolver system has been tested successfully at the operating temperature and pressure ranges of the system.

The dissolution procedure with the actual design involves pressurizing of the DNP probe to ambient pressure, leading to heating of the sample space to 4.2 K. Assuming a typical ^{13}C T_1 relaxation-rate constant of 400 s at 4.2 K, this leads to approximately 14% loss of initial polarization in the remaining samples during the dissolution process. To make the dissolutions conductible under vacuum conditions and correspondingly lower temperature, the remaining sample space needs to be sealed from the combined grabber/dissolution stick assembly. Such a design is presently under construction in our laboratory.

The multi-sample design presented here has been found to be highly convenient to conduct series of solid-state DNP experiments with varying sample compositions, since the time-consuming sample changing can be avoided.

Dissolution tests have emphasized the need for minimizing the duration of the dissolution sequence from pressurizing until dissolution. Particularly the reduction of the duration of grabbing, lifting, and sealing the sample cup to the dissolution hardware has boosted the liquid-state ^{13}C polarization levels from 10% to greater than 25%.

Acknowledgments

We would like to thank Dr. Walter Köckenberger and his group for many helpful discussions in the planning and building stages of the polarizer. Dr. Josef Granwehr also helped us with the planning of the DNP setup and especially with the LOD design. We thank Dr. Kazuyuki Takeda for supplying hardware components and valuable support for the OPENCORE NMR spectrometer. We thank Jörg Forrer for support on building the microwave circuitry. The work has been supported by following grants: ETH TH-19 07-3, SNF CR23I3_132671.

References

[1] M.A. Bouchiat, T.R. Carver, C.M. Varnum, Nuclear polarization in He-3 gas induced by optical pumping and dipolar exchange, Phys. Rev. Lett. 5 (1960) 373–375.
[2] H.U. Kauczor, R. Surkau, T. Roberts, MRI using hyperpolarized noble gases, Eur. Radiol. 8 (1998) 820–827.
[3] C.R. Bowers, D.P. Weitekamp, Para-hydrogen and synthesis allow dramatically enhanced nuclear alignment, J. Am. Chem. Soc. 109 (1987) 5541–5542.
[4] J. Natterer, J. Bargon, Parahydrogen induced polarization, Prog. Nucl. Mag. Resonan. Spectroscopy 31 (1997) 293–315.
[5] J. Haupt, New effect of dynamic polarization in a solid obtained by rapid change of temperature, Phys. Lett. A, A 38 (1972) 389.
[6] M. Tomaselli, C. Degen, B.H. Meier, Haupt magnetic double resonance, J. Chem. Phys. 118 (2003) 8559–8562.
[7] R.G. Lawler, Chemically induced dynamic nuclear polarization, J. Am. Chem. Soc. 89 (1967) 5519.
[8] A. Abragam, M. Goldman, Principles of dynamic nuclear-polarization, Rep. Prog. Phys. 41 (1978) 395–467.
[9] J.H. Ardenkjaer-Larsen, B. Fridlund, A. Gram, G. Hansson, L. Hansson, M.H. Lerche, R. Servin, M. Thaning, K. Golman, Increase in signal-to-noise ratio of >10, 000 times in liquid-state NMR, P. Natl. Acad. Sci. USA 100 (2003) 10158–10163.
[10] K. Golman, J.H. Ardenkjaer-Larsen, J.S. Petersson, S. Mansson, I. Leunbach, Molecular imaging with endogenous substances, Proc. National Academy Sci. United States Am. 100 (2003) 10435–10439.
[11] P.R. Jensen, M. Karlsson, S. Meier, J.O. Duus, M.H. Lerche, Hyperpolarized amino acids for in vivo assays of transaminase activity, Chem.-Eur. J. 15 (2009) 10010–10012.
[12] F.A. Gallagher, M.I. Kettunen, S.E. Day, D.E. Hu, J.H. Ardenkjaer-Larsen, R. in't Zandt, P.R. Jensen, M. Karlsson, K. Golman, M.H. Lerche, K.M. Brindle, Magnetic resonance imaging of pH in vivo using hyperpolarized C-13-labelled bicarbonate, Nature 453 (2008) 940–U973.
[13] R. Panek, J. Granwehr, J. Leggett, W. Kockenberger, Slice-selective single scan proton COSY with dynamic nuclear polarisation, Phys. Chem. Chem. Phys. 12 (2010) 5771–5778.
[14] L. Frydman, D. Blazina, Ultrafast two-dimensional nuclear magnetic resonance spectroscopy of hyperpolarized solutions, Nat. Phys. 3 (2007) 415–419.
[15] M. Mishkovsky, L. Frydman, Progress in hyperpolarized ultrafast 2D NMR spectroscopy, Chemphyschem 9 (2008) 2340–2348.
[16] J. Wolber, F. Ellner, B. Fridlund, A. Gram, H. Johannesson, G. Hansson, L.H. Hansson, M.H. Lerche, S. Mansson, R. Servin, M. Thaning, K. Golman, J.H. Ardenkjaer-Larsen, Generating highly polarized nuclear spins in solution using dynamic nuclear polarization, Nucl. Instrum. Meth. A 526 (2004) 173–181.
[17] A. Comment, B. van den Brandt, K. Uffmann, F. Kurdzesau, S. Jannin, J.A. Konter, P. Hautle, W.T.H. Wenckebach, R. Gruetter, J.J. van der Klink, Design and performance of a DNP prepolarizer coupled to a rodent MRI scanner, Concept Magn. Reson. B 31B (2007) 255–269.
[18] HyperSense®, Oxford instruments. <http://www.oxford-instruments.com/products/dnp/hyperSense/>.
[19] S. Jannin, A. Comment, F. Kurdzesau, J.A. Konter, P. Hautle, B. van den Brandt, J.J. van der Klink, A 140 GHz prepolarizer for dissolution dynamic nuclear polarization, J. Chem. Phys. 128 (2008).
[20] J.H. Ardenkjaer-Larsen, A.M. Leach, N. Clarke, J. Urbahn, D. Anderson, T.W. Skloss, Dynamic nuclear polarization polarizer for sterile use intent, NMR in Biomedicine (2011).
[21] J. Granwehr, J. Leggett, W. Köckenberger, A low-cost implementation of EPR detection in a dissolution DNP setup, J. Mag. Resonan. 187 (2007) 266–276.
[22] G. Whitfield, A.G. Redfield, Paramagnetic resonance detection along the polarizing field direction, Phys. Rev. 1 (1957) 918–920.
[23] A. Schweiger, R.R. Ernst, Pulsed electron-spin-resonance with longitudinal detection – a novel recording technique, J. Mag. Resonan. 77 (1988) 512–523.
[24] F. Chiarini, M. Martinelli, L. Pardi, S. Santucci, Electron-spin double resonance by longitudinal detection: Line shape and many-quantum transitions, Phys. Rev. B 12 (1975) 847–852.
[25] J.L. Du, G.R. Eaton, S.S. Eaton, Temperature orientation, and solvent dependence of electron spin-lattice relaxation rates for nitroxyl radicals in glassy solvents and doped solids, J. Mag. Resonan. Ser. A 115 (1995) 213–221.
[26] M. Martinelli, L. Pardi, C. Pinzino, S. Santucci, Electron-spin double resonance by longitudinal detection II. Signal dependence on relaxation times, Phys. Rev. B 16 (1977) 164–169.
[27] K. Takeda, A highly integrated FPGA-based nuclear magnetic resonance spectrometer, Rev. Sci. Instrum. 78 (2007).